

RESEARCH ARTICLE

10.1002/2015JA021662

MESSENGER observations of the dayside low-latitude boundary layer in Mercury's magnetosphere

Elisabet Liljeblad¹, Tomas Karlsson¹, Jim M. Raines², James A. Slavin², Anita Kullen¹, T. Sundberg³, and Thomas H. Zurbuchen²

¹Department of Space and Plasma Physics, School of Electrical Engineering, Royal Institute of Technology, Stockholm, Sweden, ²Department of Atmospheric, Oceanic and Space Sciences, University of Michigan, Ann Arbor, Michigan, USA, ³School of Physics and Astronomy, Queen Mary University of London, London, UK

Key Points:

- Investigation, characterization, and observation of the low-latitude boundary layer of Mercury
- Is there a relation between the Kelvin-Helmholtz instability and the low-latitude boundary layer
- Investigate for what surrounding conditions the low-latitude boundary layer occurs

Correspondence to:

E. Liljeblad,
elilil@kth.se

Citation:

Liljeblad, E., T. Karlsson, J. M. Raines, J. A. Slavin, A. Kullen, T. Sundberg, and T. H. Zurbuchen (2015), MESSENGER observations of the dayside low-latitude boundary layer in Mercury's magnetosphere, *J. Geophys. Res. Space Physics*, 120, 8387–8400, doi:10.1002/2015JA021662.

Received 8 JUL 2015

Accepted 13 SEP 2015

Accepted article online 19 SEP 2015

Published online 7 OCT 2015

Abstract Observations from MErcury Surface Space ENvironment GEochemistry, and Ranging (MESSENGER)'s Magnetometer and Fast Imaging Plasma Spectrometer instruments during the first orbital year have resulted in the identification of 25 magnetopause crossings in Mercury's magnetosphere with significant low-latitude boundary layers (LLBLs). Of these crossings 72% are observed dawnside and 65% for northward interplanetary magnetic field. The estimated LLBL thickness is 450 ± 56 km and increases with distance to noon. The Na⁺ group ion is sporadically present in 14 of the boundary layers, with an observed average number density of $22 \pm 11\%$ of the proton density. Furthermore, the average Na⁺ group gyroradius in the layers is 220 ± 34 km, the same order of magnitude as the LLBL thickness. Magnetic shear, plasma β and reconnection rates have been estimated for the LLBL crossings and compared to those of a control group (non-LLBL) of 61 distinct magnetopause crossings which show signs of nearly no plasma inside the magnetopause. The results indicate that reconnection is significantly slower, or even suppressed, for the LLBL crossings compared to the non-LLBL cases. Possible processes that form or impact the LLBL are discussed. Protons injected through the cusp or flank may be important for the formation of the LLBL. Furthermore, the opposite asymmetry in the Kelvin-Helmholtz instability (KHI) as compared to the LLBL rules out the KHI as a dominant formation mechanism. However, the KHI and LLBL could be related to each other, either by the impact of sodium ions gyrating across the magnetopause or by the LLBL preventing the growth of KH waves on the dawnside.

1. Introduction

The low-latitude boundary layer (LLBL) is defined at Earth as a region just inside the equatorial magnetopause with a plasma density that is intermediate between the magnetosheath and the magnetosphere values [e.g., Eastman et al., 1976; Haerendel et al., 1978; Paschmann et al., 1979; Eastman and Hones, 1979; Skopke et al., 1981]. While the mass and momentum transferred to the LLBL is estimated to be responsible for only ~10% of the total cross-magnetospheric potential [Cowley, 1982; Mozer, 1984], the existence of the LLBL is direct proof that the magnetopause is not completely impenetrable to the solar wind plasma even during northward interplanetary magnetic field (IMF).

In several important aspects Earth and Mercury are alike: they both have a similar dipolar magnetic field, where Mercury's magnetosphere is a smaller version of Earth's. Hence, many processes that occur in Earth's magnetosphere is expected to exist also in Mercury's surroundings. Due to Mercury's shorter distance to the Sun and its weaker magnetic field as compared to Earth, Hermean processes should occur faster or appear differently. Hence, Mercury's LLBL is expected to have some properties similar to Earth's but also to be different particularly when considering possible LLBL formation processes.

There are a number of observations of the Earth LLBL including larger statistical studies and case observations, particularly from the nightside region of the magnetosphere [e.g., Hones et al., 1972; Eastman et al., 1976; Slavin et al., 1985; Mitchell et al., 1987; Phan et al., 1997]. Eastman and Hones [1979] concluded that the LLBL in general occurs on closed field lines, in agreement with some case studies [e.g., Phan and Paschmann, 1996], while Mitchell et al. [1987] observed the LLBL on closed field lines for northward interplanetary magnetic field (IMF) and on a mix of open and closed field lines for southward IMF. Le et al. [1996] observed two boundaries at low latitudes during northward IMF, where the outer boundary was identified to be on open field lines and the inner one on closed.

Conclusions concerning the thickness of the terrestrial LLBL vary. *Haerendel et al.* [1978] and *Mitchell et al.* [1987] observed the LLBL to be thicker (thinner) during northward IMF (southward IMF), while *Eastman and Hones* [1979] and *Phan and Paschmann* [1996] concluded that the thickness is highly variable and shows no dependence on the IMF. Furthermore, *Mitchell et al.* [1987] and *Eastman and Hones* [1979] showed the LLBL thickness to increase with distance from noon. However, other studies revealed no such dependence [*Phan and Paschmann*, 1996]. The estimated mean Earth LLBL thickness ranges from $0.08 R_E$ to $0.6 R_E$.

The formation and entry mechanisms of the LLBL on Earth have been studied extensively, and so far several theories exist: entry via diffusion or by direct flow across the magnetopause [e.g., *Eastman et al.*, 1976; *Eastman and Hones*, 1979] where one of the proposed drivers is the Kelvin-Helmholtz (KH) instability [e.g., *Walker*, 1981; *Skopke et al.*, 1981; *Miura*, 1987], particles entering the cusp via turbulent eddy convection and subsequently drifting toward low latitudes [e.g., *Haerendel et al.*, 1978; *Müller et al.*, 2012], protons or heavy pickup ions gyrating across the magnetopause [e.g., *Slavin et al.*, 2008], random localized reconnection along the magnetopause [e.g., *Kan*, 1988; *Nishida*, 1989], reconnection near the subsolar point during southward IMF [e.g., *Fuselier et al.*, 1999], or at high latitudes equatorward of the cusps during northward IMF [e.g., *Song and Russell*, 1992; *Le et al.*, 1996; *Øieroset et al.*, 2008]. Some of these mechanisms should lead to asymmetries in the plasma composition of the LLBL, which may be particularly relevant at Mercury. Heavy pickup ions from the solar wind or magnetosheath that will drift in opposite directions for northward (dawnward) and southward (duskward) IMF should create an asymmetry in mass loading related to the direction of the IMF. Moreover, protons that have entered the magnetopause through diffusion or have been injected through the cusp or the flank will drift dawnward on closed field lines due to the gradient-curvature drift, which should lead to an IMF-independent occurrence asymmetry [e.g., *Anderson et al.*, 2011]. In case the KH instability is responsible for the formation of the LLBL on Mercury, the boundary layer should appear mainly during northward IMF at the duskside magnetopause [*Liljeblad et al.*, 2014].

The observations of the dayside LLBL (both near 6 MLT) on Mercury from the two flybys, M1 and M2, [*Slavin et al.*, 2008] have been analyzed by *Wang et al.* [2010], *Anderson et al.* [2011], and *Müller et al.* [2012]. Both flybys crossed the LLBL on the dawnside but for different IMF directions (northward during M1 and southward during M2). Despite the different conditions during the two flybys, the characteristics were similar for both boundary layers. At the downstream magnetopause *Slavin et al.* [2012] identified a wide LLBL very similar to that observed at the Earth [e.g., *Slavin et al.*, 1985] for strong, steady northward plasma sheet magnetic field just inside the magnetopause. No comprehensive statistical study on the Mercury LLBL exists so far.

In a recent statistical study of the KH instability on Mercury by *Liljeblad et al.* [2014], a distinct dawn-dusk asymmetry was observed, where the KH waves occurred more often on the duskside magnetopause. The same asymmetry was indicated in previous smaller studies [*Boardsen et al.*, 2010; *Sundberg et al.*, 2012]. Moreover, the study showed that the large majority of the KH waves occurred for northward IMF. Different theories explain the asymmetry observed, where two are connected either to an asymmetric mass loading in the velocity shear layer where the KH instability forms [e.g., *Anderson et al.*, 2011; *Sundberg and Slavin*, 2015] or to the finite Larmor radius (FLR) effects and the broadening of the shear layer on the dawnside magnetopause [e.g., *Glassmeier and Espley*, 2006; *Nakamura et al.*, 2010; *Gershman et al.*, 2015; *Gingell et al.*, 2015]. However, the asymmetry is still viewed as an open issue, and both theories need to be confirmed by further observations. Therefore, one of the motivations for this study is to establish whether or not there is a connection between the asymmetry in the KH wave occurrence and the observed LLBL on Mercury.

The present study aims at a systematic analysis of the magnetopause crossings carried out by the Mercury Surface Space ENvironment GEOchemistry, and Ranging (MESSENGER) spacecraft during the year 2011, to identify Mercury's LLBL and estimate its properties. Formation processes will be discussed on the basis of estimations of the plasma and magnetic field in the magnetosheath near the magnetopause. This includes the comparison to a control group consisting of distinct magnetopause crossings that show a lack of plasma on the magnetospheric side of the boundary, from now on referred to as non-LLBL crossings.

2. Data Analysis

The investigation of magnetopause crossings has been performed using magnetic field and plasma data from the Magnetometer (MAG) [*Anderson et al.*, 2007] and the Fast Imaging Plasma Spectrometer (FIPS) [*Andrews et al.*, 2007] instruments on board MESSENGER. The data analyzed was collected during year 2011, i.e., from 26 March 2011 to 31 December 2011, covering slightly more than three Mercury years (~ 88 days) of data.

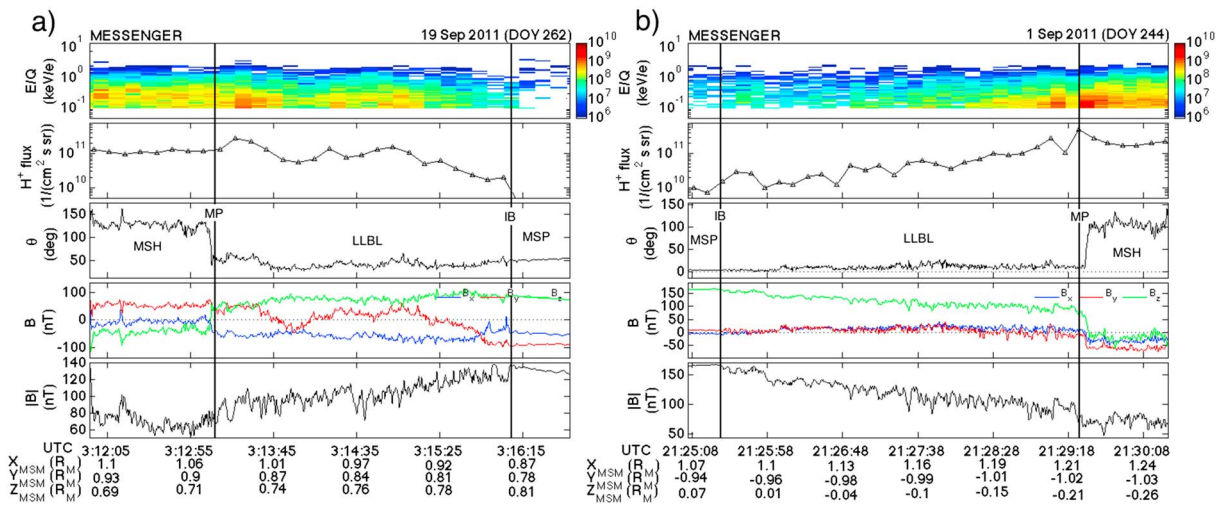


Figure 1. Two examples of magnetopause crossings with an LLBL present on (a) an inbound and (b) outbound trajectory. The inner boundary (IB) and the magnetopause (MP) are marked with solid black lines. From top to bottom: (first panel) A proton energy spectrogram, (second panel) the total proton flux, (third panel) the polar angle (angle from the magnetic north pole axis) of the magnetic field, (fourth panel) B_x (blue), B_y (red), B_z (green) in MSM coordinates, and (fifth panel) the total magnetic field. When crossing the MP from the magnetosheath (MSH), there is a distinct change in magnetic field direction, followed by a gradual decrease in proton counts across the LLBL. The fluctuations in the magnetic field and the proton flux decrease as the spacecraft moves across the inner boundary layer and into the magnetosphere (MSP).

This was before the orbit period was lowered from 12 h to 8 h in April 2012. After April 2012, the LLBL was significantly less frequently observed when using the criteria displayed in section 2.2, most likely due to MESSENGER crossing the equatorial magnetopause differently as compared to before the orbit change. Hence, only the three first Mercury years of data from year 2011 was used in this study. MESSENGER's orbit in MSM coordinates (\hat{x} is directed from the center of the planetary dipole toward the Sun, \hat{z} points in the general direction of the north magnetic pole, and \hat{y} completes the right-handed system) during year 2011 can be seen in Figure 1. MESSENGER covers the Hermean magnetosphere almost symmetrically during 2011, and as far back on the flank as $x_{MSH} = -2 R_M$, where R_M (~ 2440 km) is one Mercury radius.

The non-LLBL crossings are by definition different from the LLBL group as they lack magnetosheath plasma inside the magnetopause. It is therefore of interest to investigate if the surrounding conditions for these two groups, such as the state of the plasma and magnetic field near the magnetopause, are different. Hence, the non-LLBL crossings will serve as a reference to the LLBL group.

A third set of data considered in this study for comparison is 28 nonlinear KH waves during 2011 that have been identified and analyzed by Liljeblad *et al.* [2014].

2.1. Description of Measurements

The MAG instrument has a resolution of 0.047 nT at a rate of 20 samples per second. The FIPS instrument is a time-of-flight (TOF) mass spectrometer that measures mass per charge (m/q) with a range of 1 to 60 amu e^{-1} and energy per charge (E/q) from 0.1(0.05) to 13 keV/e of incident ions with a scan time of approximately 10 s (1 min) inside (outside) the magnetosphere [Andrews *et al.*, 2007]. The conical instantaneous field of view (FOV) of FIPS is 1.4π sr and reduced to 1.15π sr due to obstruction by the spacecraft and the sunshade. For a more detailed description of the FIPS FOV limitations, including its impact on measured parameters, see Raines *et al.* [2011, 2013] and Gershman *et al.* [2012, 2013].

Parameters such as the plasma number density and temperature are considered in this study. The calculation of these plasma moments with the FIPS measurements assumes that the observed distribution is hot and isotropic and that the thermal speed is large compared to the bulk flow speed, which are not always applicable to regions such as the magnetosheath [e.g., Raines *et al.*, 2011; Gershman *et al.*, 2013]. However, in the regions within 3 h local time of the subsolar point, these assumptions produce reasonable estimates when hydrodynamic flow conditions are assumed [Spreiter *et al.*, 1966]. Additional details are given below.

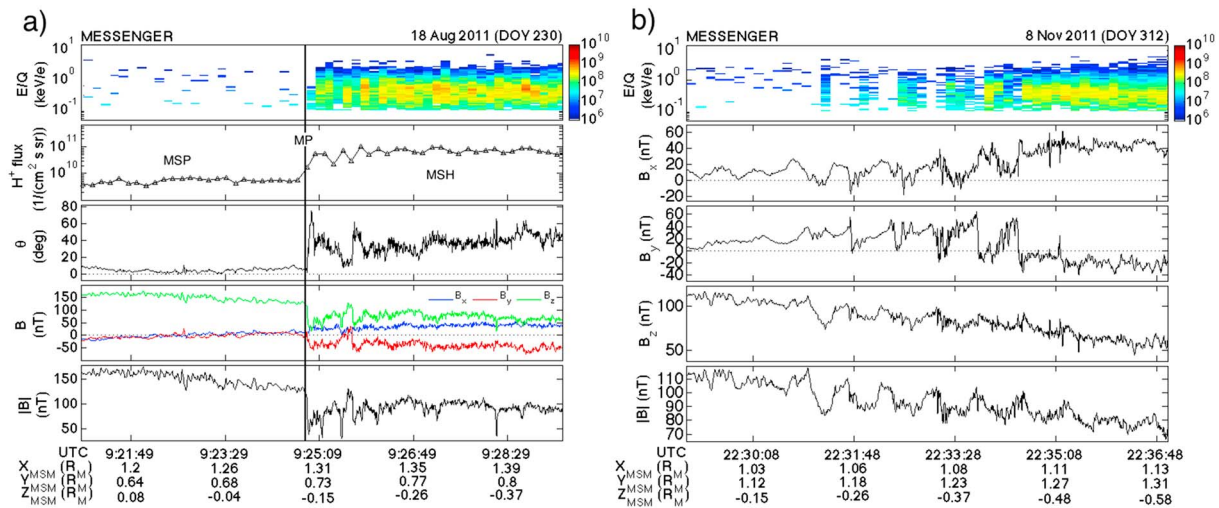


Figure 2. Examples of a (a) non-LLBL crossing and (b) KH event in its nonlinear phase. As the spacecraft moves across the MP from the MSH, there is a distinct change in magnetic field direction. A clear depletion of plasma on the magnetospheric side of the MP can be observed. For the nonlinear KH event, a typical sawtooth signature is visible, particularly in the B_y component. Additional panel details are explained in Figure 2.

2.2. Characterization of Magnetopause Crossings

An LLBL is identified if there is a region of magnetosheath plasma inside the magnetopause, with a distinguishable inner boundary and magnetopause (outer boundary). For an outbound crossing, the magnetopause is identified when fulfilling two out of three of the following criteria:

1. Distinct magnetic field rotation across the boundary.
2. Distinct increase in H^+ counts for typical magnetosheath energies ($\sim 0.1 - 3$ keV).
3. Increase in magnetic field fluctuations.

For an inbound crossing, the inner boundary must fulfill two out of three of the following criteria:

1. Distinct increase in H^+ counts for typical magnetosheath energies.
2. Increase in magnetic field fluctuations.
3. Decrease of total magnetic field strength.

For an inbound crossing, the boundaries are defined analogously. In a dense plasma a decrease of the total magnetic field at the inner boundary is expected as a diamagnetic response to an increase in particle flux. Moreover, plasma often give rise to fluctuations in the magnetic field.

Two examples of LLBL crossings can be seen in Figure 2. On an inbound crossing of the magnetopause in Figure 2a, (outbound in Figure 2b), marked with a solid black line, the magnetic field direction changes abruptly along with a gradual decrease in proton counts across the LLBL. When the spacecraft reaches the inner boundary and eventually traversing into the magnetosphere, the proton flux is reduced further and fluctuations diminish.

Magnetopause crossings are identified as non-LLBL if they show very little or no plasma inside the magnetopause and fulfill the same criteria for the magnetopause as the LLBL events do.

An example of a non-LLBL crossing and a nonlinear KH event can be seen in Figure 3. The magnetopause marks the region where there is a noticeable change in both proton flux and polar angle of the magnetic field. In addition, the clear lack of plasma on the inner side of the magnetopause is readily distinguishable. A sawtooth structure, characteristic for a nonlinear KH wave [e.g., Hasegawa *et al.*, 2004] can be seen most clearly in the B_y panel of the KH event.

2.3. Evaluation of Magnetic Field and Plasma Properties Near the Magnetopause

On Earth, there is a clear correlation between reconnection and southward IMF [e.g., Fairfield and Cahill, 1966; Arnoldy, 1971]. Moreover, observations show that when the magnetosheath plasma $\beta \ll 2$, the likeliness of reconnection increases [e.g., Paschmann *et al.*, 1986]. Particularly, reconnection during low magnetic shear

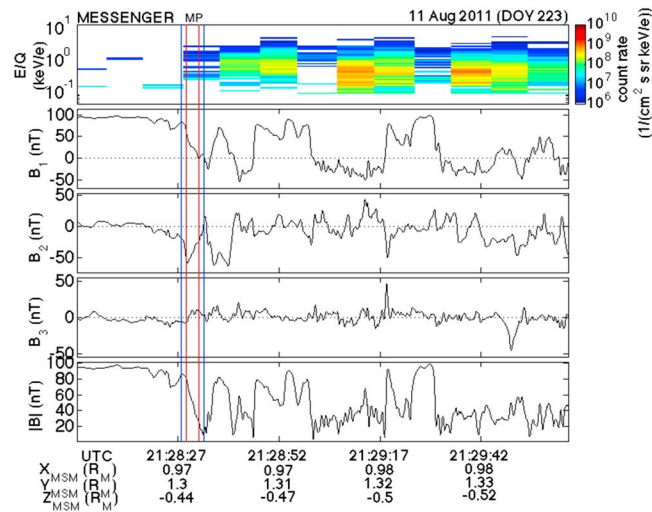


Figure 3. An example of a non-LLBL crossing in MVA coordinates, with a successful normal determination. From top to bottom, (first panel) A proton energy spectrogram and (second to fifth panels) the magnetic field data. B_1 is the maximum variance, B_2 the intermediate, and B_3 the minimum variance coordinates. The magnetopause crossing, marked with blue lines, have a normal of $\hat{n} = (0.74, -0.45, 0.50)$, an eigenvalue ratio of $\lambda_2/\lambda_3 = 22$, and $|B_N| = 6.3$ nT. The red lines mark a slightly shortened interval of the magnetopause crossing, with $\hat{n} = (0.71, -0.40, 0.57)$, $\lambda_2/\lambda_3 = 9.4$, and $|B_N| = 8.8$ nT.

(the angle between the direction of the magnetic field prior to and after a magnetopause crossing) has been observed mainly when the magnetosheath β is low [e.g., Scurry et al., 1994].

Due to the short time separation between MESSENGER’s passage across the magnetopause and its measurement of the LLBL, analysis of the state of the magnetic field should give reliable estimations of reconnection rates at the time of the LLBL formation. In turn, this investigation may indicate how the LLBL was formed. The investigation includes the estimation of magnetic shear and reconnection rate across the magnetopause, the plasma β in the magnetosheath just prior to/after the magnetopause crossing, and the number density of plasma within the LLBL.

Direct calculation of reconnection rates has turned out to be difficult at Earth [e.g., Sonnerup and Scheible, 1998; Paschmann et al., 2014]. Moreover, Mercury is highly dynamic which may make it even more difficult to estimate the reconnection rates there. To reduce errors in the estimation, certain criteria will be used, as explained in the following section.

2.3.1. Determination of the Reconnection Rate

The reconnection rate is approximated by the expression $B_N/|B|$, where B_N is the magnetic field component normal to the magnetopause and $|B|$ the total magnetic field just inside the magnetopause [Sonnerup et al., 1981; DiBraccio et al., 2013]. The magnetopause normal is determined using minimum variance analysis (MVA) on the magnetopause crossings [Sonnerup and Cahill, 1967].

As a first criterion, we only consider those magnetopause crossings that are well determined, i.e., show an intermediate to minimum variance eigenvalue ratio larger than 3. In some cases, the exact position of a complete magnetopause crossing can be difficult to determine. Moreover, the MVA can be highly sensitive to the intervals chosen for analysis. Hence, as a second criterion we only consider reconnection rates for those events with a distinct transition across the magnetopause with a normal that does not vary considerably when making small adjustments to the interval analyzed. When multiple magnetopause crossings can be observed, the one closest to the magnetosphere is chosen. The reconnection rates calculated from the full crossings (not partial) are always used to represent the true reconnection rate. Figure 4 displays an example of a non-LLBL crossing in MVA coordinates with an accepted normal determination, where B_1 is the maximum variance, B_2 the intermediate, and B_3 the minimum variance coordinates. Red lines mark a shortened interval of the complete magnetopause crossing, indicated with blue lines. The larger interval has a normal of $\hat{n} = (0.74, -0.45, 0.50)$, an eigenvalue ratio of $\lambda_2/\lambda_3 = 22$, and a normal magnetic field $|B_N| = 6.3$ nT. In turn, the shortened interval has $\hat{n} = (0.71, -0.40, 0.57)$, $\lambda_2/\lambda_3 = 9.4$, and $|B_N| = 8.8$ nT. This yields a reconnection rate of 0.07 for the full crossing and 0.10 for the shorter time period, both similar to each other and below the average reconnection rates of 0.15 observed previously on Mercury [DiBraccio et al., 2013; Slavin et al., 2009].

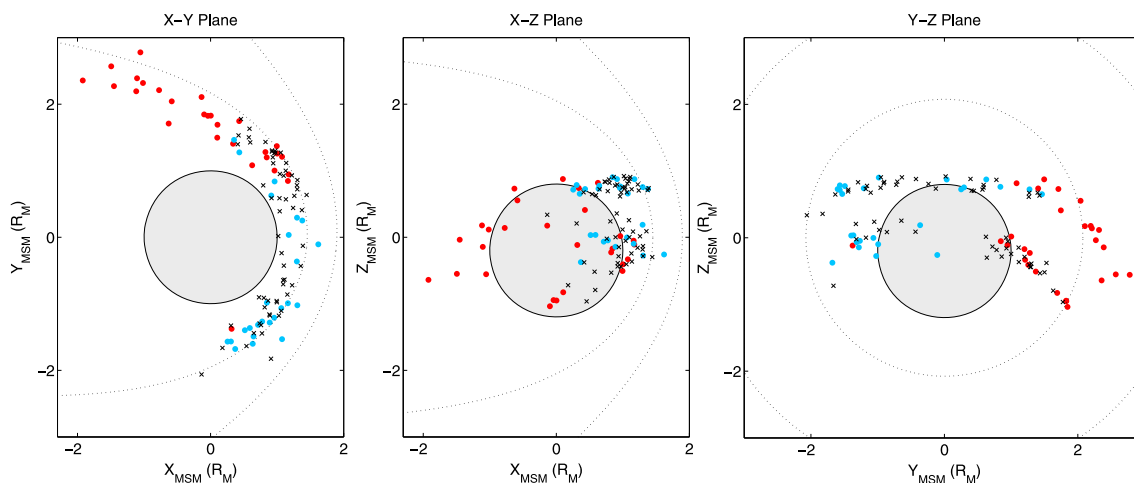


Figure 4. Location of LLBL crossings (blue dots), nonlinear KH waves (red dots), and non-LLBL crossings (black crosses) projected onto the (a) y - x , (b) z - x , and (c) z - y planes in MSM coordinates. Inner and outer dashed lines are the estimated magnetopause and bow shock, respectively.

2.3.2. Estimation of the Plasma β in the Magnetosheath

The plasma β is defined as $\beta = \frac{nk_B T}{B/2\mu_0}$, where n and T are the number density and temperature for the plasma, respectively, k_B is the Boltzmann constant, and μ_0 is the magnetic field permeability of free space. It has been calculated directly from measurements of protons and the magnetic field in the magnetosheath just prior to/after crossing the magnetopause. As the FIPS instrument has a limited FOV, the plasma density and temperature are obtained by using a forward modeling approach relying on the assumption that the thermal speed of H^+ ions is larger than the bulk flow speed [e.g., Raines et al., 2011]. Away from the subsolar point, the bulk flow speed of the magnetosheath gradually increases, and the forward modeling approach will give larger errors. In particular, within 45° from noon, the errors will not affect the β estimates by more than 50%. Hence, in this study the β estimate is restricted to those magnetopause crossings occurring within 9–15 MLT.

3. Observations

The analysis of magnetic field and plasma data from MESSENGER during year 2011 resulted in the identification of 25 LLBL and 61 non-LLBL crossings. These two groups will be used, together with 28 nonlinear KH waves from the year 2011 that have been identified in Liljeblad et al. [2014], to analyze and characterize the dayside Hermean LLBL.

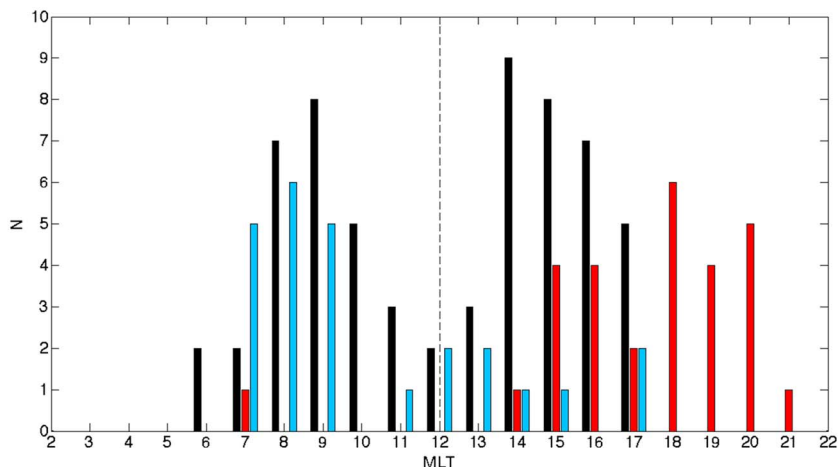


Figure 5. MLT histogram of LLBL crossings (blue), nonlinear KH waves (red), and non-LLBL crossings (black). The dashed line marks the subsolar point in this and subsequent figures.

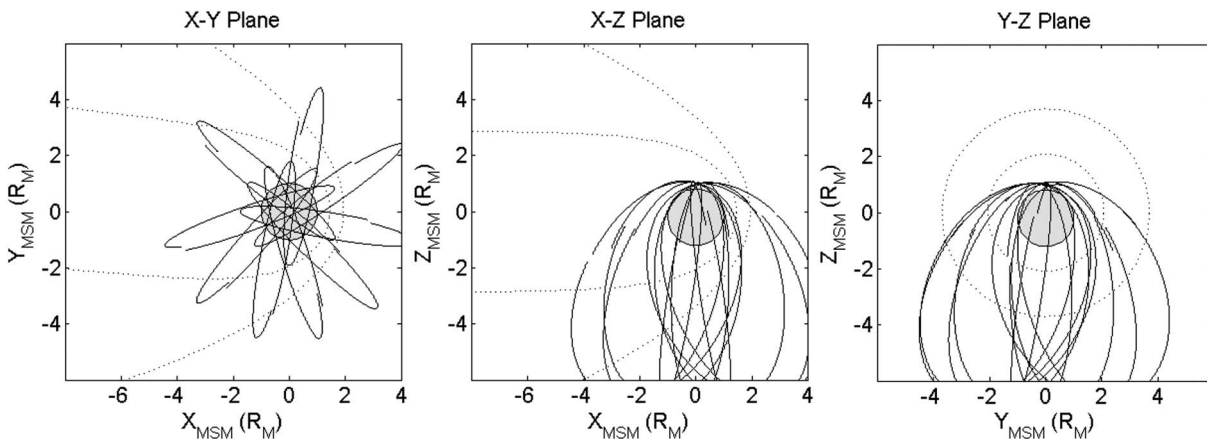


Figure 6. Nine selected orbits of MESSENGER during one Mercury year in 2011 projected onto the (a) y - x , (b) z - x , and (c) z - y planes in MSM coordinates [Liljeblad et al., 2014].

3.1. Location

Figure 5 shows the position of the LLBL crossings (blue dots), the non-LLBL crossings (black crosses), and nonlinear KH waves (red dots) projected into three different planes in MSM coordinates. The MLT histogram plot for the three groups with the same color coding can be seen in Figure 6. Of the LLBL crossings, 72% occur on the dawnside magnetopause, while the nonlinear KH waves are highly overrepresented at the duskside (93%). The non-LLBL crossings, however, show no such asymmetry and are nearly equally distributed over the dayside magnetopause, except near the subsolar point where almost no events are observed. The reason for this dip for the non-LLBL crossings could possibly be due to an orbital effect or an increased difficulty in determining the position of the magnetopause in this region. The anticorrelation of occurrence between the LLBL and KH instability indicates that the majority of the boundary layers observed are not formed by the KH instability, but rather by another process.

Even though MESSENGER covers the Hermean magnetosphere fairly symmetrically during 2011 and parts of the equatorial magnetosphere behind the dawn-dusk terminator (see Figure 1), all of the LLBL and non-LLBL crossings occur sunward of the dawn-dusk terminator. This is, again, likely related to an orbital effect making it more difficult to determine the position of the magnetopause far away from noon. For that reason, only the dayside LLBL on Mercury has been covered in this study.

3.2. Surrounding Conditions

To determine the state of the magnetopause just prior to/after the crossing of an LLBL or non-LLBL, magnetic shear, reconnection rate and plasma β have been estimated.

The magnetosheath B_z distribution over MLT can be seen in Figure 7. The majority of the LLBL events show a positive magnetosheath B_z /northward IMF (65%), while the non-LLBL events are observed mostly for negative

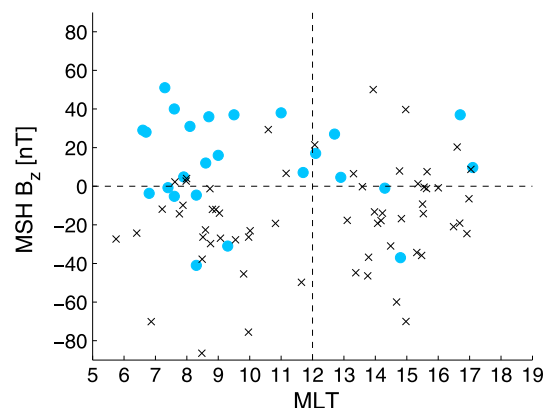


Figure 7. Magnetosheath B_z versus MLT for the LLBL (blue dots) and non-LLBL (black crosses) magnetopause crossings.

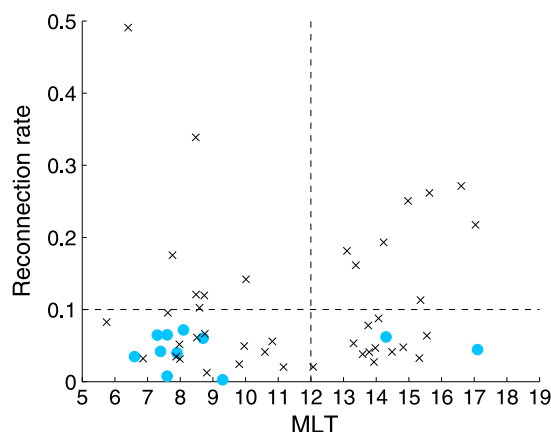


Figure 8. Reconnection rates versus MLT for LLBL (blue dots) and non-LLBL (black crosses) crossings. The horizontal line marks the reconnection rate of 0.10.

B_z (77%). This can be compared to the observations of the Hermean nonlinear KH waves, where 89% occurs for northward IMF [Liljeblad et al., 2014]. Furthermore, the average shear angle for the LLBL group is $67^\circ \pm 8^\circ$, which is significantly lower than the mean shear angle for non-LLBL crossings ($120^\circ \pm 6^\circ$).

Performing an MVA on the magnetopause crossing and the criteria described in section 2.3.1, reconnection rates could be determined for 11 out of 25 LLBL crossings, and for 41 out of 61 non-LLBL crossings. Figure 8 displays how the reconnection rates vary with MLT for the two groups. The mean reconnection rates are 0.05 ± 0.01 and 0.11 ± 0.02 for the LLBL and non-LLBL crossings, respectively. These values are smaller than previous estimates of Hermean reconnection rates of ~ 0.15 [DiBraccio et al., 2013; Slavin et al., 2014], but particularly for the non-LLBL crossings the reconnection rates are larger than what has generally been observed at Earth, < 0.1 [e.g., Sonnerup and Ledley, 1979; Phan et al., 2001; Vaivads et al., 2004]. In particular, all crossings with reconnection rates > 0.10 are non-LLBL crossings.

By restricting the estimation of plasma β to events within 9–15 MLT, as described in section 2.3.2, β was calculated for 9 LLBL and 29 non-LLBL crossings. The average β of these LLBL and non-LLBL crossings are 2.0 ± 0.4 and 4.4 ± 0.7 , respectively. The β was approximated by using only the proton pressure. Alpha particle pressures were omitted because these ions were typically not present in sufficient numbers to allow pressure calculations for all LLBL and non-LLBL cases considered. When pressures could be computed, alpha particles typically increase the plasma β by 30–50%. This does not change our conclusion that the plasma pressure is clearly dominating the magnetic pressure. Heavier ions were not present in sufficient numbers to justify pressure calculations for these.

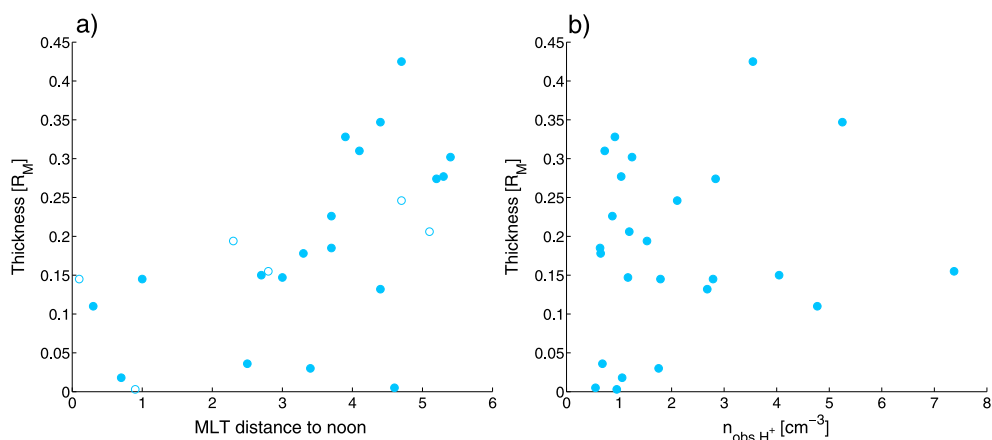


Figure 9. (a) Thickness of duskside (circles) and dawnside (filled circles) LLBLs projected onto the surface model normal by Shue et al. [1997] versus MLT distance to noon. (b) Thickness versus observed proton density.

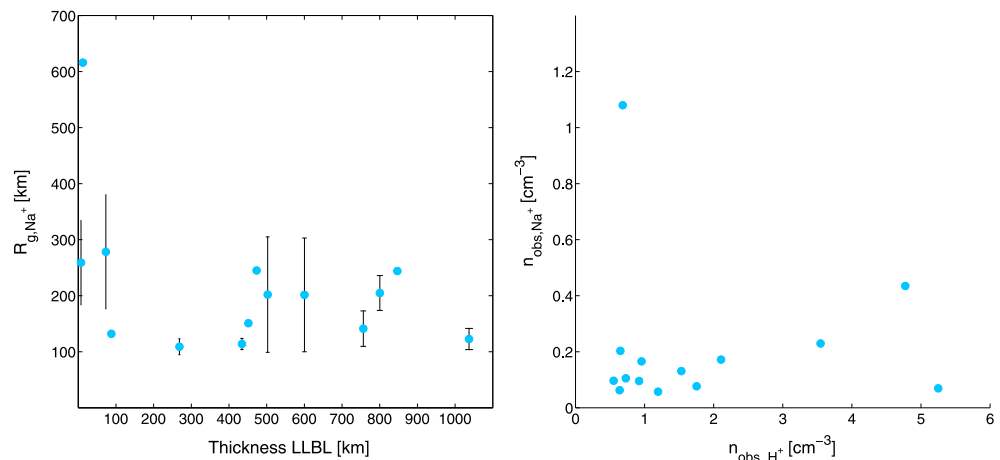


Figure 10. A comparison between (left) the average Na⁺ group gyroradius in the LBL and the estimated LBL thickness, including error bars for the gyroradii estimations, and (right) the average observed number density for the Na⁺ group and H⁺ ions. Both panels include properties only on those 14 LBLs with a nonnegligible Na⁺ group number density.

3.3. LBL Characteristics

The average proton number density in the LBLs is $26 \pm 5 \text{ cm}^{-3}$, which is higher than both of the estimated densities for the dayside boundary layers observed during M1 and M2, which were 16 cm^{-3} and 8 cm^{-3} , respectively [Raines *et al.*, 2011]. Assuming that the plasma in the LBL is nearly stagnant, the average β in the LBL has been estimated to 0.36 ± 0.05 , indicating that the magnetic field is dominating the plasma pressure in the boundary layers.

The thickness of the LBL has been determined by projecting the spacecraft LBL trajectory onto the Shue *et al.* [1997] magnetopause normal direction using a subsolar standoff distance $1.45 R_M$ and magnetopause flaring parameter 0.5 [Winslow *et al.*, 2013; Slavin *et al.*, 2014]. The average LBL thickness is $0.18 \pm 0.02 R_M$ ($450 \pm 56 \text{ km}$) with no distinct dependence on IMF direction, in agreement with some Earth observations [e.g., Eastman and Hones, 1979; Phan and Paschmann, 1996]. Moreover, no relation between magnetosheath B_x or B_y and the LBL thickness could be found. However, in Figure 9a, the LBL thickness appears to increase with distance to the subsolar point, consistent with what has been reported for the LBL at Earth [Haerendel *et al.*, 1978; Eastman and Hones, 1979]. No dependence is seen between the thickness and the distance to the equatorial plane or the magnetic latitude, indicating that the observed correlation is not likely an orbital effect. Furthermore, in Figure 9b the thickness of the LBL shows no clear dependence of the average observed number density in the boundary layers.

The thickness for dawnside- and duskside-observed LBL crossings are $0.20 \pm 0.03 R_M$ and $0.14 \pm 0.04 R_M$, respectively. This difference is, however, probably related to the boundary layer being wider away from noon, as the dawnside LBL crossings are seen more frequently farther away from the subsolar point (peaking at 7–9 MLT), while the duskside LBL crossings are more equally distributed between 12 and 17 MLT (see Figure 5).

The LBL is frequently populated by ions heavier than protons, in particular by He²⁺ and Na⁺ group ions. The phase space density for each measured ion was added into one of 20 logarithmically spaced gyroradius bins to form particle distributions as a function of gyroradius, $f(r_g)$. Average and standard deviation values of the gyroradius were then computed from these distributions in the usual manner for the first and second velocity moments, with the velocity coordinate replaced by gyroradius. Unlike the protons, the sodium group ions are not continuously present throughout the boundary layer. Instead, they are identified sporadically in the LBL. In general, however, these ions are near the detection limit, meaning that they could be present in the LBL in a more continuous way, but as the FIPS is unable to detect them most of the time, they are only measured sporadically. When the Na⁺ group ions do appear in specifically 14 out of 25 boundary layers, their number density is significantly large (at least 3% of the average observed proton number density in the LBL). For these 14 LBL crossings, the average Na⁺ group gyroradius was estimated to $220 \pm 34 \text{ km}$, which is in the same order of magnitude as the mean thickness of these LBL ($440 \pm 63 \text{ km}$). Slavin *et al.* [2008] estimated a gyroradius of $\sim 1000 \text{ km/s}$ for a Na⁺ ion picked up by the solar wind flowing with a speed of 300 km/s , corresponding to the thickness of the dayside boundary layer observed from M1. The Na⁺ group ion gyroradii observed in this

study are significantly smaller than that. However, their gyroradii are similar to that of a sodium ion moving with a velocity of 50 km/s in a magnetosheath of 50 nT magnetic field strength. A comparison between the LLBL width and the average sodium group gyroradius is displayed in Figure 10 (left). The observed number density for these 14 LLBL crossings, displayed in Figure 10 (right), is significantly smaller for Na⁺ group ions as compared to the H⁺ ions. For only one of these events, the sodium group is dominating. On average, however, the sodium group has a number density of $22 \pm 11\%$ of the proton number density.

The average H⁺ gyroradius in the boundary layer is 40 ± 4 km, significantly smaller than the average LLBL thickness. However, for five LLBL crossings the boundary layer width is similar to the proton gyroradius.

4. Discussion

The majority of the LLBL crossings are observed at the dawnside, which indicates that the formation process acts differently on Mercury as compared to Earth, where no such dawn-dusk asymmetry is observed [e.g., Haerendel *et al.*, 1978; Eastman and Hones, 1979; Phan and Paschmann, 1996; Le *et al.*, 1996]. The KH instability has been suggested to play an important role in the formation of the LLBL at Earth [e.g., Walker, 1981; Sckopke *et al.*, 1981; Miura, 1987]. However, the distinct anticorrelation between the nonlinear KH waves and the LLBL on Mercury rules out the KH instability as an important mechanism for the formation of the Hermean LLBL.

As the IMF is northward for the majority of LLBL crossings, and the reconnection rates are nonnegligible ($0.05 \pm .01$), high-latitude reconnection is a possible LLBL formation process. There have been suggestions that high-latitude reconnection gives rise to multiple boundary layers at low latitudes [e.g., Song and Russell, 1992; Le *et al.*, 1996], with one or more boundary layers being on closed field lines. This theory relies on the assumption that the same magnetic field line gets reconnected poleward of the cusp in both hemispheres. Reconnection could also occur in an alternating fashion, accelerating plasma toward lower latitudes and forming an LLBL not consisting of several boundary layers, but instead of one with accelerated magnetosheath plasma. In any event, high-latitude reconnection should lead to a high energetic plasma population inside the LLBL, that is distinguishable from the magnetosheath plasma [e.g., Le *et al.*, 1996]. Such an increase in energy relative to the magnetosheath is not observed for any of the LLBL crossings. Hence, high-latitude reconnection is not likely an important LLBL formation mechanism on Mercury.

The reason why the non-LLBL crossings are nearly void of plasma just inside the magnetopause, even though reconnection is likely ongoing, is not obvious. However, it may be the result of ongoing fast reconnection, rapidly accelerating and dragging away the reconnected plasma from the *X* line toward the cusp in a way that MESSENGER is unable to detect it. This is supported by the large shear angles and reconnection rates of the non-LLBL as compared to the LLBL crossings. Even though the estimated average β for the non-LLBL crossings is large (4.4 ± 0.7), the magnetic shear is likely often high enough to trigger reconnection and give rise to the large reconnection rates. In turn, the smaller reconnection rates and magnetic shear in combination with a relatively large β for the LLBL crossings (2.0 ± 0.4) suggest that fast reconnection is not ongoing. Rather, it is more likely that plasma gets transferred across the magnetopause either through slow reconnection or by a completely different process.

The plasma depletion layer (PDL), defined as a region on the dayside in the magnetosheath of decreased plasma density and increased magnetic field, is believed to occur when the solar wind Alfvénic Mach number is low [e.g., Zwan and Wolf, 1976] and can enhance reconnection [DiBraccio *et al.*, 2013; Gershman *et al.*, 2013]. Gershman *et al.* [2013] studied the Hermean PDL for 40 MESSENGER orbits, where flux pileup was seen to occur for all IMF orientations. Prior to two of the LLBL crossings identified in this study, the PDL was observed. Even though it is unlikely that these LLBLs have been formed directly through processes in the magnetosheath, they could have been formed by plasma from the magnetosphere. In any case, if the PDL had a large impact on the formation of the LLBL, the β in the magnetosheath prior to the magnetopause crossing should be low, which is not, in general, observed.

Müller *et al.* [2012] proposed that a double current sheet at the dayside on Mercury may exist in a pure solar wind hydrogen plasma, without any contribution of exospheric ions like sodium. The diamagnetic decrease at the inner boundary is explained to arise due to pressure gradients from protons that have entered at the dawn flank and become trapped on closed magnetic field lines. Similar effects should arise if the particles enter through the cusp. Korth *et al.* [2014] further showed the existence of an enhanced plasma population

near the magnetopause flanks, due to direct entry of magnetosheath plasma, and a higher flux of protons on the dawnside. This LLBL formation theory is consistent not only with the observed dawn-dusk asymmetry in the LLBL, which should arise due to the gradient-curvature drift of these trapped protons, but also with the observed lower reconnection rates and magnetic shears in combination with the large β . This process should, however, also give rise to a dawn-dusk asymmetry in the Earth LLBL, which is not observed. As Mercury has a significantly smaller magnetosphere than Earth, and processes occur more rapidly, the Hermean LLBL could get populated in a short enough time by these trapped protons and form a distinguishable LLBL. This may, however, not be the case at Earth where protons need longer time to travel along closed field lines between the two hemispheres. To determine whether or not the Hermean LLBL protons are on closed field lines, further detailed investigation of the LLBL plasma is needed. This would include assumptions and simplifications due to limitations in the FIPS instrument, which is outside the scope of this study.

The estimated thickness of the LLBL is observed to increase with distance to noon, in agreement with some observations at Earth [e.g., Mitchell *et al.*, 1987; Eastman and Hones, 1979]. No dependence on the thickness with distance to the equatorial plane was found, indicating that it is not an effect arising from MESSENGER's orbit. However, Phan and Paschmann [1996] showed that when only considering the duration of the crossings, there was a clear difference between the LLBL observed for a high- and low-shear magnetopause. Although, when taking the magnetopause motion into account (the high-shear LLBL magnetopause motion moved twice as fast as the low-shear one), the discrepancy was removed. There is no relation between the Hermean LLBL width and magnetic shear, or the magnetic shear and distance to noon. In particular, the magnetic shear does not decrease away from the subsolar point. All this suggest that the LLBL does indeed become broader away from the subsolar point, possibly by some diffusive mechanism. What has not been considered is the Shue *et al.* [1997] model's effect on the thickness estimations. The model normal may differ more from the real magnetopause further away from noon and could possibly have an impact on the thickness approximation. How this will alter the thickness or its dependence on distance from noon, however, is unclear. The observed number density shows no clear correlation with the thickness of the LLBL. Particularly for the boundary layers with a number density smaller than 3 cm^{-3} , there is an insignificant difference in number density for different LLBL thicknesses, indicating that the boundary layers are continuously fed by protons along the whole dayside.

At Earth, the proton gyroradius is estimated to be significantly smaller than the LLBL thickness [e.g., Le *et al.*, 1996]. On Mercury, however, the majority of the estimated average Na^+ group ion gyroradii in the LLBL are of the same order of magnitude as the average LLBL thickness. Formation of the LLBL by ions gyrating across the magnetopause should give rise to the observed dawn-dusk asymmetry in the LLBL, either due to the solar wind convection electric field driving the ions toward dawn for northward IMF or as a result of the gradient-curvature drift of protons, independent on the IMF, that have ended up on closed field lines due to a scattering process. This theory agrees with the study by Raines *et al.* [2013], which concluded that Na^+ ions are more frequently observed on the dawnside, sunward of the dawn-dusk terminator where the majority of the LLBLs are found. The ion gyroradii observed in this study ($220 \pm 34 \text{ km}$) are significantly smaller than that of a sodium ion picked up by the solar wind; however, they do compare to the sodium gyroradius in a nearly stagnant magnetosheath. The sodium group ions are only measured sporadically throughout the LLBL. However, as they are near the detection limit, they could indeed be continuously present throughout the LLBL. Moreover, when they are observed, their number density are often high enough to make the sodium group ion the dominant species in mass density in that specific region. It is difficult to evaluate the sodium group ions impact on the LLBL from these measurements, but the fact that they are measured sporadically with a significant number density for 14 out of 25 LLBLs demonstrate that they are at least not insignificant for the LLBL formation. The proton gyroradii in the LLBLs are in general considerably smaller than the mean LLBL width, indicating that the gyration of the magnetosheath protons are probably not important for the LLBL formation. However, as they are present in large number densities continuously throughout all LLBLs, the protons should naturally be considered as highly important for the LLBL formation.

That the IMF is northward for the majority of events for both LLBL crossings and KH waves raises the question whether or not there is a common reason for the observed dawn-dusk asymmetries. Theories [Glassmeier and Espley, 2006] and simulations [e.g., Nakamura *et al.*, 2010] predict Na^+ ions to have a significant impact on the velocity shear layer and the KH instability on Mercury, by suppressing the growth rate of KH waves on the dawnside for northward IMF. In turn, sodium ions in the magnetosheath may gyrate across the magnetopause to form the LLBL. In particular, the ions should, in the magnetosheath, gyrate in the dawnward

direction during northward IMF, thus possibly giving rise to the observed dawn-dusk asymmetry in the LLBL. However, if sodium ions form the LLBL, we would expect the LLBL to occur also at the duskside for southward IMF. This is not observed, which suggests that there might be another process present that inhibits the formation of a steady LLBL for southward IMF. Such a process could be fast reconnection, rapidly dragging the reconnected plasma away from the X line, as discussed previously. Indeed, fast reconnection should be anticipated particularly during southward IMF when magnetic shear is large. The only time that reconnection should be suppressed on Mercury, or at least proceed with a lower rate, is when magnetic shear is low enough and β significantly large. As discussed previously, rapid reconnection is most likely not ongoing for the dawnside LLBL events due to the combination of lower reconnection rates and small magnetic shears as compared to the non-LLBL, and the relatively large β . A difficulty with this theory is the observation of protons: the identification of the LLBL is based on magnetic field and plasma data from H^+ ions only. Furthermore, the average observed number density of the Na^+ group in the boundary layers is in general small, as compared to the H^+ number density. One possible explanation to this observation is that the Na^+ ions broaden the thickness of the LLBL enough on the dawnside to be clearly distinguishable when applying the criteria in section 2.2. Another possibility is Na^+ ions affecting the presence of H^+ ions in the LLBL. The idea of sodium having a large impact on the magnetospheric boundaries would indeed explain both the dawn-dusk asymmetry for both the LLBL and KH instability and some related observations of the surrounding conditions.

Another idea is that the LLBL and KH wave anticorrelation is due to the LLBL broadening the velocity shear layer where the KH instability grows. Again, that the LLBL is observed mainly during northward IMF and on the dawnside agrees well with this. As previously explained, several mechanisms and formation processes could give rise to this LLBL dawn-dusk asymmetry on the dayside of Mercury, whereas the same processes at Earth would work differently and have a smaller impact on the LLBL formation.

5. Summary

Observations from MESSENGER's MAG and FIPS instruments during year 2011 have resulted in the identification of 25 magnetopause crossings with significant LLBLs. These occur mainly on the dawnside (72%) and for northward IMF (65%).

The approximated thickness of the LLBL, with an average of 450 ± 56 km, is observed to increase from the subsolar point. The sodium group ions are observed sporadically in the LLBL, unlike the protons that are present throughout the whole boundary layer. When observed, the sodium group ions have a number density slightly more than 20% of the proton number density, with an average gyroradius of 220 ± 34 km. Hence, the average Na^+ group gyroradius is on the same order of magnitude as the LLBL thickness.

The LLBL-estimated average magnetic shear, reconnection rate, and plasma β are $67^\circ \pm 34^\circ$, $0.05^\circ \pm 0.01^\circ$, and $2.0^\circ \pm 0.4^\circ$, respectively. These values have been compared to a control group containing 61 distinct magnetopause crossings with nearly no plasma inside the magnetopause. The results indicate that reconnection is slower for the LLBL group or maybe even suppressed in some cases as compared to the non-LLBL crossings and earlier estimations of Hermean reconnection rates.

Based on these results, different LLBL formation mechanisms have been discussed. Results indicate that the boundary layers are continuously fed by protons along the whole dayside. Furthermore, the idea of particles injected through the cusp or at the magnetopause flanks, drifting downward on closed field lines and eventually populating the LLBL [e.g., Müller *et al.*, 2012], agrees with the observations in this study and could possibly be an important LLBL formation mechanism. As shown in Liljeblad *et al.* [2014], nonlinear KH waves on Mercury are mainly observed at the duskside magnetopause. Hence, the KH instability is ruled out as a likely LLBL formation process. Both the LLBL and KH waves occur for northward IMF, indicating either that one mechanism may be responsible for the opposite dawn-dusk asymmetry between the two or that the LLBL suppresses the growth rate of the KH instability on the dawnside. Theories and simulations have predicted the Na^+ ions to have a significant effect on the velocity shear layer, mainly by suppressing the growth rate of the KH instability on the dawnside [e.g., Glassmeier and Espley, 2006; Nakamura *et al.*, 2010]. Similarly, the Na^+ ions could possibly induce a dawn-dusk asymmetry in the LLBL, as the Na^+ ions should drift downward during northward IMF, making the LLBL more populated by heavy ions on this side of the magnetopause. Alternatively, the asymmetry in LLBL mass loading, in combination with them being observed mainly during northward IMF, suggest that the LLBL could be directly responsible for the KH wave dawn-dusk asymmetry by broadening the shear layer on the dawnside and thereby restricting the growth of the KH waves there.

Acknowledgments

This work was partially supported by the Swedish National Space Board and the University of Michigan. The data for this paper are available at the NASA Planetary Data System: planetary plasma interactions node archive (<http://pds-ppi.igpp.ucla.edu>).

Yuming Wang thanks two reviewers for their assistance in evaluating this paper.

References

- Anderson, B. J., M. H. Acuña, D. A. Lohr, J. Scheifele, A. Raval, H. Korth, and J. A. Slavin (2007), The magnetometer instrument on MESSENGER, *Space Sci. Rev.*, *131*(1–4), 417–450.
- Anderson, B. J., J. A. Slavin, H. Korth, S. A. Boardsen, T. H. Zurbuchen, J. M. Raines, G. Gloeckler, R. L. McNutt, and S. C. Solomon (2011), The dayside magnetospheric boundary layer at Mercury, *Planet. Space Sci.*, *59*(15), 2037–2050.
- Andrews, G. B., et al. (2007), The energetic particle and plasma spectrometer instrument on the MESSENGER spacecraft, *Space Sci. Rev.*, *131*(1–4), 523–556.
- Arnoldy, R. L. (1971), Signature in the interplanetary medium for substorms, *J. Geophys. Res.*, *76*(22), 5189–5201.
- Boardsen, S. A., T. Sundberg, J. A. Slavin, B. J. Anderson, H. Korth, S. C. Solomon, and L. G. Blomberg (2010), Observations of Kelvin-Helmholtz waves along the dusk-side boundary of Mercury's magnetosphere during MESSENGER's third flyby, *Geophys. Res. Lett.*, *37*, L12101, doi:10.1029/2010GL043606.
- Cowley, S. (1982), The causes of convection in the Earth's magnetosphere: A review of developments during the IMS, *Rev. Geophys.*, *20*(3), 531–565.
- DiBraccio, G. A., J. A. Slavin, S. A. Boardsen, B. J. Anderson, H. Korth, T. H. Zurbuchen, J. M. Raines, D. N. Baker, R. L. McNutt, and S. C. Solomon (2013), MESSENGER observations of magnetopause structure and dynamics at Mercury, *J. Geophys. Res. Space Physics*, *118*, 997–1008, doi:10.1002/jgra.50123.
- Eastman, T., and E. Hones (1979), Characteristics of the magnetospheric boundary layer and magnetopause layer as observed by IMP 6, *J. Geophys. Res.*, *84*(A5), 2019–2028.
- Eastman, T., E. Hones, S. Bame, and J. Asbridge (1976), The magnetospheric boundary layer: Site of plasma, momentum and energy transfer from the magnetosheath into the magnetosphere, *Geophys. Res. Lett.*, *3*(11), 685–688.
- Fairfield, D. H., and L. Cahill (1966), Transition region magnetic field and polar magnetic disturbances, *J. Geophys. Res.*, *71*(1), 155–169.
- Fuselier, S., M. Lockwood, T. Onsager, and W. Peterson (1999), The source population for the cusp and cleft/LLBL for southward IMF, *Geophys. Res. Lett.*, *26*(12), 1665–1668.
- Gershman, D. J., T. H. Zurbuchen, L. A. Fisk, J. A. Gilbert, J. M. Raines, B. J. Anderson, C. W. Smith, H. Korth, and S. C. Solomon (2012), Solar wind alpha particles and heavy ions in the inner heliosphere observed with MESSENGER, *J. Geophys. Res.*, *117*, A00M02, doi:10.1029/2012JA017829.
- Gershman, D. J., J. A. Slavin, J. M. Raines, T. H. Zurbuchen, B. J. Anderson, H. Korth, D. N. Baker, and S. C. Solomon (2013), Magnetic flux pileup and plasma depletion in Mercury's subsolar magnetosheath, *J. Geophys. Res. Space Physics*, *118*, 7181–7199, doi:10.1002/2013JA019244.
- Gershman, D. J., J. M. Raines, J. A. Slavin, T. H. Zurbuchen, T. Sundberg, S. A. Boardsen, B. J. Anderson, H. Korth, and S. C. Solomon (2015), MESSENGER observations of multiscale Kelvin-Helmholtz vortices at Mercury, *J. Geophys. Res. Space Physics*, *120*, 4354–4368, doi:10.1002/2014JA020903.
- Gingell, P. W., T. Sundberg, and D. Burgess (2015), The impact of a hot sodium ion population on the growth of the Kelvin-Helmholtz instability in Mercury's magnetotail, *J. Geophys. Res. Space Physics*, *120*, 5432–5442, doi:10.1002/2015JA021433.
- Glassmeier, K.-H., and J. Espley (2006), ULF waves in planetary magnetospheres, in *Magnetospheric ULF Waves: Synthesis and New Directions*, edited by K. Takahashi et al., pp. 341–359, AGU, Washington, D. C.
- Haerendel, G., G. Paschmann, N. Sckopke, H. Rosenbauer, and P. Hedgecock (1978), The frontside boundary layer of the magnetosphere and the problem of reconnection, *J. Geophys. Res.*, *83*(A7), 3195–3216.
- Hasegawa, H., M. Fujimoto, T.-D. Phan, H. Reme, A. Balogh, M. Dunlop, C. Hashimoto, and R. TanDokoro (2004), Transport of solar wind into Earth's magnetosphere through rolled-up Kelvin-Helmholtz vortices, *Nature*, *430*(7001), 755–758.
- Hones, E. W., J. Asbridge, S. Bame, M. Montgomery, S. Singer, and S.-I. Akasofu (1972), Measurements of magnetotail plasma flow made with Vela 4B, *J. Geophys. Res.*, *77*(28), 5503–5522.
- Kan, J. (1988), A theory of patchy and intermittent reconnections for magnetospheric flux transfer events, *J. Geophys. Res.*, *93*(A6), 5613–5623.
- Korth, H., B. J. Anderson, D. J. Gershman, J. M. Raines, J. A. Slavin, T. H. Zurbuchen, S. C. Solomon, and R. L. McNutt (2014), Plasma distribution in Mercury's magnetosphere derived from messenger magnetometer and fast imaging plasma spectrometer observations, *J. Geophys. Res. Space Physics*, *119*, 2917–2932, doi:10.1002/2013JA019567.
- Le, G., C. Russell, J. Gosling, and M. Thomsen (1996), ISEE observations of low-latitude boundary layer for northward interplanetary magnetic field: Implications for cusp reconnection, *J. Geophys. Res.*, *101*(A12), 27,239–27,249.
- Liljeblat, E., T. Sundberg, T. Karlsson, and A. Kullen (2014), Statistical investigation of Kelvin-Helmholtz waves at the magnetopause of Mercury, *J. Geophys. Res. Space Physics*, *119*, 9670–9683, doi:10.1002/2014JA020614.
- Mitchell, D., F. Kutchko, D. Williams, T. Eastman, L. Frank, and C. Russell (1987), An extended study of the low-latitude boundary layer on the dawn and dusk flanks of the magnetosphere, *J. Geophys. Res.*, *92*(A7), 7394–7404.
- Miura, A. (1987), Simulation of Kelvin-Helmholtz instability at the magnetospheric boundary, *J. Geophys. Res.*, *92*(A4), 3195–3206.
- Mozer, F. (1984), Electric field evidence on the viscous interaction at the magnetopause, *Geophys. Res. Lett.*, *11*(2), 135–138.
- Müller, J., S. Simon, Y.-C. Wang, U. Motschmann, D. Heyner, J. Schüle, W.-H. Ip, G. Kleindienst, and G. J. Pringle (2012), Origin of Mercury's double magnetopause: 3D hybrid simulation study with AIKEF, *Icarus*, *218*(1), 666–687.
- Nakamura, T., H. Hasegawa, and I. Shinohara (2010), Kinetic effects on the Kelvin-Helmholtz instability in ion-to-magnetohydrodynamic scale transverse velocity shear layers: Particle simulations, *Phys. Plasmas*, *17*(4), 042119.
- Nishida, A. (1989), Can random reconnection on the magnetopause produce the low latitude boundary layer?, *Geophys. Res. Lett.*, *16*(3), 227–230.
- Øieroset, M., T. Phan, V. Angelopoulos, J. Eastwood, J. McFadden, D. Larson, C. Carlson, K.-H. Glassmeier, M. Fujimoto, and J. Raeder (2008), THEMIS multi-spacecraft observations of magnetosheath plasma penetration deep into the dayside low-latitude magnetosphere for northward and strong by IMF, *Geophys. Res. Lett.*, *35*, L17S11, doi:10.1029/2008GL033661.
- Paschmann, G., N. Sckopke, G. Haerendel, J. Papamastorakis, S. Bame, J. Asbridge, J. Gosling, E. Hones Jr., and E. Tech (1979), ISEE plasma observations near the subsolar magnetopause, in *Advances in Magnetospheric Physics with GEOS-1 and ISEE*, edited by K. Knott, A. Durney, and K. Ogilvie, pp. 397–417, Springer, Netherlands.
- Paschmann, G., I. Papamastorakis, W. Baumjohann, N. Sckopke, C. Carlson, B. Sonnerup, and H. Lüher (1986), The magnetopause for large magnetic shear: AMPTE/IRM observations, *J. Geophys. Res.*, *91*(A10), 11,099–11,115.
- Paschmann, G., M. Øieroset, and T. Phan (2014), In-situ observations of reconnection in space, in *Microphysics of Cosmic Plasmas*, edited by A. Balogh et al., pp. 309–341, Springer, New York.
- Phan, T., et al. (1997), Low-latitude dusk flank magnetosheath, magnetopause, and boundary layer for low magnetic shear: Wind observations, *J. Geophys. Res.*, *102*(A9), 19,883–19,895.

- Phan, T. D., and G. Paschmann (1996), Low-latitude dayside magnetopause and boundary layer for high magnetic shear: 1. Structure and motion, *J. Geophys. Res.*, *101*(A4), 7801–7815.
- Phan, T. D., B. U. Sonnerup, and R. P. Lin (2001), Fluid and kinetics signatures of reconnection at the dawn tail magnetopause: Wind observations, *J. Geophys. Res.*, *106*(A11), 25,489–25,501.
- Raines, J. M., J. A. Slavin, T. H. Zurbuchen, G. Gloeckler, B. J. Anderson, D. N. Baker, H. Korth, S. M. Krimigis, and R. L. McNutt (2011), MESSENGER observations of the plasma environment near Mercury, *Planet. Space Sci.*, *59*(15), 2004–2015.
- Raines, J. M., et al. (2013), Distribution and compositional variations of plasma ions in Mercury's space environment: The first three Mercury years of MESSENGER observations, *J. Geophys. Res. Space Physics*, *118*, 1604–1619, doi:10.1029/2012JA018073.
- Sckopke, N., G. Paschmann, G. Haerendel, B. Sonnerup, S. Bame, T. Forbes, E. Hones, and C. Russell (1981), Structure of the low-latitude boundary layer, *J. Geophys. Res.*, *86*(A4), 2099–2110.
- Scurry, L., C. Russell, and J. Gosling (1994), Geomagnetic activity and the beta dependence of the dayside reconnection rate, *J. Geophys. Res.*, *99*(A8), 14,811–14,814.
- Shue, J.-H., J. Chao, H. Fu, C. Russell, P. Song, K. Khurana, and H. Singer (1997), A new functional form to study the solar wind control of the magnetopause size and shape, *J. Geophys. Res.*, *102*(A5), 9497–9511.
- Slavin, J., E. Smith, D. Sibeck, D. Baker, R. Zwickl, and S.-I. Akasofu (1985), An ISEE 3 study of average and substorm conditions in the distant magnetotail, *J. Geophys. Res.*, *90*(A11), 10,875–10,895.
- Slavin, J. A., et al. (2008), Mercury's magnetosphere after MESSENGER's first flyby, *Science*, *321*(5885), 85–89.
- Slavin, J. A., et al. (2009), MESSENGER observations of magnetic reconnection in Mercury's magnetosphere, *Science*, *324*(5927), 606–610.
- Slavin, J. A., et al. (2012), MESSENGER and Mariner 10 flyby observations of magnetotail structure and dynamics at Mercury, *J. Geophys. Res.*, *117*, A01215, doi:10.1029/2011JA016900.
- Slavin, J. A., et al. (2014), MESSENGER observations of Mercury's dayside magnetosphere under extreme solar wind conditions, *J. Geophys. Res. Space Physics*, *119*, 8087–8116, doi:10.1002/2014JA020319.
- Song, P., and C. Russell (1992), Model of the formation of the low-latitude boundary layer for strongly northward interplanetary magnetic field, *J. Geophys. Res.*, *97*(A2), 1411–1420.
- Sonnerup, B., and L. Cahill (1967), Magnetopause structure and attitude from Explorer 12 observations, *J. Geophys. Res.*, *72*(1), 171–183.
- Sonnerup, B., and B. Ledley (1979), Ogo 5 magnetopause structure and classical reconnection, *J. Geophys. Res.*, *84*(A2), 399–405.
- Sonnerup, B., G. Paschmann, I. Papamastorakis, N. Sckopke, G. Haerendel, S. Bame, J. Asbridge, J. Gosling, and C. Russell (1981), Evidence for magnetic field reconnection at the Earth's magnetopause, *J. Geophys. Res.*, *86*(A12), 10,049–10,067.
- Sonnerup, B. U., and M. Scheible (1998), Minimum and maximum variance analysis, in *Analysis Methods for Multi-Spacecraft Data*, edited by G. Paschmann and P. Daly, pp. 185–220, ESA/ISSI, Paris.
- Spreiter, J. R., A. L. Summers, and A. Y. Alksne (1966), Hydrodynamic flow around the magnetosphere, *Planet. Space Sci.*, *14*, 223–253.
- Sundberg, T., and J. A. Slavin (2015), Mercury's magnetotail, in *Magnetotails in the Solar System*, edited by A. Keiling, C. M. Jackman, and P. A. Delamere, pp. 33–34, John Wiley, Hoboken, N. J.
- Sundberg, T., S. A. Boardsen, J. A. Slavin, B. J. Anderson, H. Korth, T. H. Zurbuchen, J. M. Raines, and S. C. Solomon (2012), MESSENGER orbital observations of large-amplitude Kelvin-Helmholtz waves at Mercury's magnetopause, *J. Geophys. Res.*, *117*, A04216, doi:10.1029/2011JA017268.
- Vaivads, A., Y. Khotyaintsev, M. André, A. Retino, S. Buchert, B. Rogers, P. Décréau, G. Paschmann, and T. Phan (2004), Structure of the magnetic reconnection diffusion region from four-spacecraft observations, *Phys. Rev. Lett.*, *93*(10), 105001.
- Walker, A. (1981), The Kelvin–Helmholtz instability in the low-latitude boundary layer, *Planet. Space Sci.*, *29*(10), 1119–1133.
- Wang, Y.-C., J. Mueller, U. Motschmann, and W.-H. Ip (2010), A hybrid simulation of Mercury's magnetosphere for the MESSENGER encounters in year 2008, *Icarus*, *209*(1), 46–52.
- Winslow, R. M., B. J. Anderson, C. L. Johnson, J. A. Slavin, H. Korth, M. E. Purucker, D. N. Baker, and S. C. Solomon (2013), Mercury's magnetopause and bow shock from MESSENGER magnetometer observations, *J. Geophys. Res. Space Physics*, *118*(5), 2213–2227.
- Zwan, B., and R. Wolf (1976), Depletion of solar wind plasma near a planetary boundary, *J. Geophys. Res.*, *81*(10), 1636–1648.